

Fig. 1: The network model as a Gilbert graph: streets (thin lines) are represented by a PVT; devices (dots) are positioned uniformly at random on the streets; edges (thick lines) are drawn whenever two devices are separated by less than a connectivity threshold  $r > 0$ .

- 3) How many hops per unit of distance are necessary to connect two devices in the same connected component?

The network model used for the simulations is described in Section II. The simulation methods are described in Section III. Results and discussion follow in Section IV.

## II. NETWORK MODEL

Following [10], [11], we model a street system  $T$  as a PVT or PDT based on a planar Poisson point process. Note that, with reference to the conditions presented in [12], these street systems are stabilising and asymptotically essentially connected. In particular, we do not consider Poisson line tessellations, which are not stabilising. We denote by  $\gamma = \mathbb{E}[\nu_1(T \cap [-1/2, 1/2]^2)]$  the length intensity of  $T$  where  $\nu_1$  measures the one-dimensional total length of  $T$  in the unit square  $[-1/2, 1/2]^2$ . For a street system in a given city or part of a city, it is possible to obtain the best fitting tessellation process and the corresponding value of  $\gamma$  easily using the statistical tools presented in [8].

For any realisation  $T$  of the street system, devices are distributed according to a one-dimensional Poisson point process  $X$  with intensity measure  $\lambda\nu_1(T \cap du)$  where  $\lambda > 0$  is a scalar parameter. In other words, the number of devices in an area  $A$  is a Poisson random variable with parameter  $\lambda\nu_1(T \cap A)$  and each device is placed independently and uniformly in  $T \cap A$ . In short,  $X$  is a Cox point process with random intensity measure  $\lambda\nu_1(T \cap du)$ .

As in [3], we assume the communication radius between devices to be constant, so that we can construct the communication graph as a Gilbert graph with radius  $r > 0$ . The answer to the first question presented in the introduction then amounts to finding the critical percolation threshold  $\lambda_c$  of this Gilbert graph.

Answering the second question amounts to tracing the percolation function  $\lambda \mapsto \theta(\lambda, r, \gamma)$  where

$$\theta(\lambda, r, \gamma) = \mathbb{P}(o \rightsquigarrow \infty)$$

is the Palm probability, that a randomly selected user is connected to infinity in the Gilbert graph.

Finally, in view of sub-additivity of the number of hops and the corresponding results on the Poisson Boolean model (PBM), see [13], it is reasonable to assume the existence of a deterministic stretch factor  $\mu(\lambda, r, \gamma) > 1/r$  given by

$$\lim_{\substack{X_i, X_j \rightsquigarrow \infty \\ |X_i - X_j| \rightarrow \infty}} \frac{S(X_i, X_j)}{|X_i - X_j|} = \mu(\lambda, r, \gamma).$$

Here,  $S(x, y)$  denotes the smallest number of hops from  $x$  to  $y$  and we assume  $\lambda > \lambda_c$ . Therefore, the answer to the third question will consist in tracing the curves  $\lambda \mapsto \mu(\lambda, r, \gamma)$  for given  $r$  and  $\gamma$ .

The model presented here exhibits a scaling invariance: Changing  $\gamma$  to  $a\gamma$  is equivalent to zooming to a larger or smaller window for the original  $\gamma$  value, thus changing  $\lambda$  to  $a\lambda$  and  $r$  to  $r/a$ . Consequently, we considered only two dimensionless parameters, namely  $\lambda/\gamma$  and  $r\gamma$ , for the simulations, and will switch back to three parameters when necessary in order to present the results in physical terms.

While the inclusion of a statistically realistic model for the city layout is a major step forward, three important simplifying assumptions are still required:

- 1) The transmission power of devices is a global constant.
- 2) Signal shadowing and fading effects due to the urban landscape are neglected.
- 3) Interference between devices is not taken into account.

## III. METHODOLOGY

In order to answer the three key questions raised in Section I, we rely on Monte Carlo estimates of three key quantities: the critical percolation threshold, the percolation probability and the stretch factor. First, the critical percolation threshold is needed to decide whether long-range multi-hop communication is possible at all. Second, the percolation probability describes the proportion of devices in an unbounded connected component : this gives the probability for a given device to be able to communicate on a long-range scale. Third, the stretch factor determines how many hops are needed to cover a given large distance.

### A. Critical percolation thresholds

The first problem we encounter with simulations is to estimate infinite connected components in finite windows. To tackle this problem, we realize the tessellations on a torus. Thereby the left side and the right side of the window as well as the up and bottom sides could adjust perfectly; see Figure 2. In order to do that, we simply generate a Poisson point process in the finite window, and then copy the points from a large band on the left of the window to the right, and correspondingly from the bottom to the top of the window.

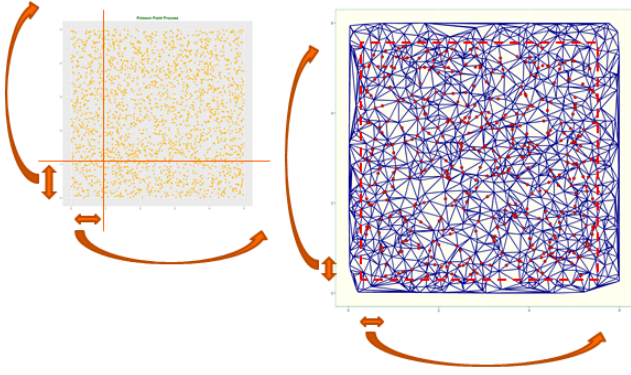


Fig. 2: Tracing on a torus : after plotting a planar Poisson process in a  $5\text{km} \times 5\text{km}$  window, the points on the left are copied to the right and the points at the bottom are copied to the top. The corresponding PDT is traced and the dotted line in red thus delimits a  $5\text{km} \times 5\text{km}$  window representing the torus. The devices (red dots) could then be placed uniformly at random on the edges of the graph inside the window, and the devices in a band on the left or at the bottom are copied to the right and top.

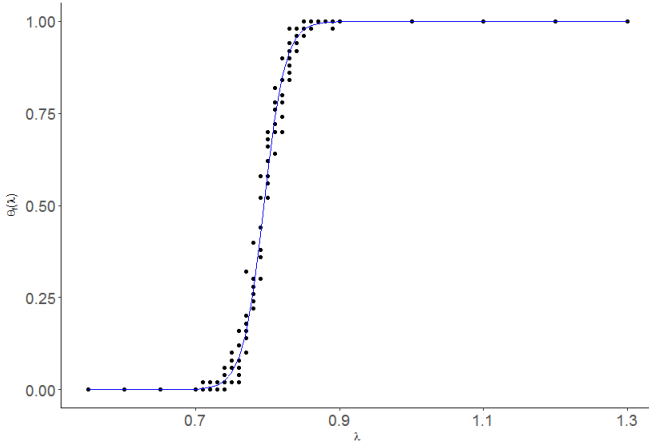


Fig. 3: Proportion of simulations where we find an infinite component as a function of  $\lambda$ . Each point represents an estimate for a given  $\lambda$ . The blue line represents the logistic regression curve.

In order to avoid boundary effects, we then generate devices uniformly at random on the streets in a sub-window in the center of the extended window, and copy the devices from the left and bottom sides of the window to the right and up sides. Infinite connected components then correspond to components that cross the window, either from left to right or from top to bottom, joining a user to its copy.

Figure 3 shows the estimate of the proportion of simulations  $p$  where we find an infinite component as a function of  $\lambda$ . The logistic model  $\log(p/(1-p)) = a\lambda + b$  seems to perfectly fit the curve. Finding  $a$  and  $b$  by linear regression, it is then possible

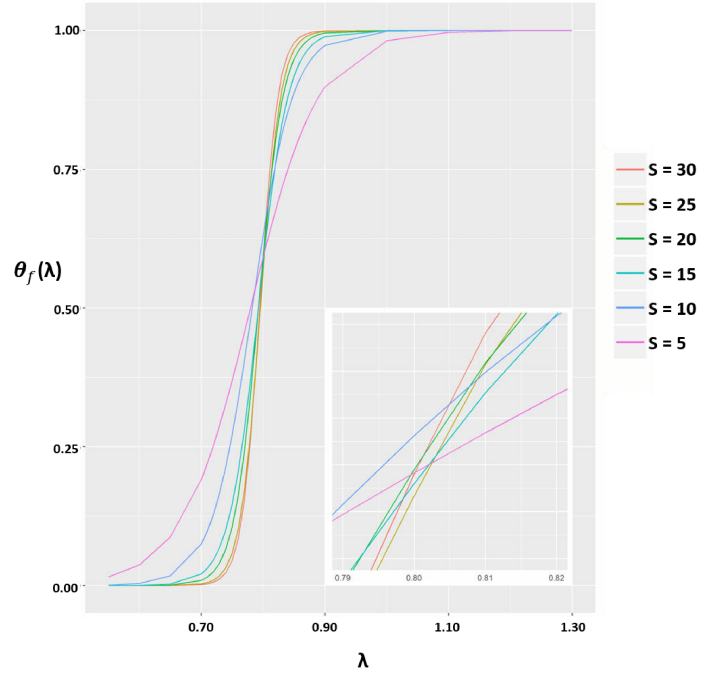


Fig. 4: Tracing curves  $\lambda \mapsto p(\lambda)$  for window sizes varying between  $5\text{km} \times 5\text{km}$  and  $30\text{km} \times 30\text{km}$ : the curves intersect near  $p = 0.6$ .

to obtain the value of  $\lambda$  for a given  $p$ . Figure 4 presents the logistic curves for varying window sizes. First, we observe that as the simulation windows grow, the curves tend to the theoretical function of the percolation probability (in the limit when the window's size goes to infinity, the  $p(\lambda)$  function is 0 for  $\lambda < \lambda_c$  and 1 for  $\lambda > \lambda_c$ ). Second, we observe that all the curves cross in a limited region around  $p = 0.6$ , thus, we approximate  $\lambda_c$  via

$$\lambda_c \approx (\log(0.6/0.4) - b)/a.$$

### B. Percolation probabilities

In order to calculate the percolation probabilities we use the following algorithm. First, for a realisation  $t$  of the random tessellation, we start by selecting the origin  $o$  uniformly from the street system. Then, we add points sequentially on the street system, again following the uniform distribution. For each new point, we use the union-find algorithm, see [14], in order to update the connected components of the Gilbert graph. We stop adding points as soon as the connected component containing the origin crosses the window from a point to its copy. For each tessellation  $t_k, k = 1, \dots, n$  we run the simulation of point placements  $M$  times and for the  $i$ th such simulation we denote by  $N_{k,i}$  the number of points needed to exhibit the window crossing.

Let  $\{o \rightsquigarrow \partial W\}$  denote the event that zero is contained in a connected component which crosses the window  $W$ . Further,

let  $J$  denote the number of points of the process  $X$  of devices in the simulation window and let

$$\theta_t = \sum_{j>0} \mathbb{P}(o \rightsquigarrow \partial W | J = j, T = t) \mathbb{P}(J = j | T = t)$$

so that the expected value of  $\theta_T$  (with respect to the tessellation process  $T$ ) is a finite-volume estimator of  $\theta$ .

For given a realisation of the street system  $T = t$  the number of devices is Poisson distributed with mean  $\lambda\nu_1(t)$  and hence

$$\mathbb{P}(J = j | T = t) = \exp(-\lambda\nu_1(t)) \frac{\lambda^j \nu_1(t)^j}{j!}.$$

Moreover, since each tessellation realisation is assigned equal weight and since the property of percolation is stable with respect to the addition of further devices, a natural estimator for  $\theta$  is

$$\hat{\theta}(\lambda) = \frac{1}{n} \sum_{k \leq n} \frac{1}{M} \sum_{i \leq M} \sum_{j \geq N_{k,i}} e^{-\lambda\nu_1(t_k)} \frac{\lambda^j \nu_1(t_k)^j}{j!}. \quad (1)$$

The sum  $\sum_{j \geq N_{k,i}} e^{-\lambda\nu_1(t_k)} \frac{\lambda^j \nu_1(t_k)^j}{j!}$  equals  $\mathbb{P}(J \geq N_{k,i} | T = t_k)$  and is therefore simply one minus the cumulative distribution function for a Poisson random variable with known mean and thus readily available from computational libraries. Note that each simulation will give a value for  $N_{k,i}$ , and then values of  $\hat{\theta}$  for different  $\lambda$  can be computed from (1) without extra simulations.

### C. Stretch factor

Since we must have an infinite connected component, we consider only values  $\lambda > \lambda_c$ . In order to compute the stretch factor for each  $\lambda$  value, we first determine the chemical distance, i.e., the minimal number of hops between two devices for all pairs in a given simulation via the Floyd-Warshall algorithm [15]. Then, we compute the Euclidean distance between each pair of points. Since  $\mu$  is a limit for large distance only pairs with distance more than 4km in a window of side length 5km are taken into account for the estimation.

## IV. RESULTS

We now present the results of the Monte Carlo experiments described in the previous sections. Simulations were performed in the statistical computing environment R [16]. Unless stated differently, the street system length intensity is fixed to  $\gamma = 20\text{km}^{-1}$  which corresponds to dense urban areas.

### A. Estimation of the percolation threshold

The observation window for the simulations is fixed to  $30\text{km} \times 30\text{km}$  unless stated otherwise. For certain parameter combinations the window size had to be reduced due to computational constraints.

Table I shows the various critical values found for  $\lambda/\gamma$ , allowing to compute  $\lambda_c$  for various values of  $\gamma$  for PDT and PVT models, to be compared to the standard Poisson Boolean Model (PBM). The simulations for  $r\gamma = 1.5$  were performed on a  $15\text{km} \times 15\text{km}$  window, those for  $r\gamma = 0.5$

TABLE I: Percolation threshold  $\lambda_c/\gamma$  as function of  $r\gamma$ .

$r\gamma$	$\lambda_c/\gamma$		
	PVT	PDT	PBM
0.3	11.9	12.4	15.95
0.5	5.58	5.83	5.74
1.5	0.75	0.79	0.638
2.5	0.24	0.26	0.229
3.5	0.12	0.13	0.117
4.5	0.071	0.075	0.0709
5.5	0.048	0.049	0.0474
6.5	0.034	0.035	0.034
7.5	0.025	0.026	0.0255
8.5	0.0199	0.0202	0.01995
9.5	0.0159	0.0159	0.0159

and those for  $r\gamma = 0.3$  on a  $10\text{km} \times 10\text{km}$  window. Note that a comparison with the critical intensity for the PBM leads to the approximation

$$\lambda_c \gamma^{-1} \approx 4.51 \pi^{-1} (r\gamma)^{-2},$$

see [17, Table 2].

For a standard city centre,  $\gamma \approx 20\text{km}^{-1}$ , so that if  $r = 0.475\text{km}$ , we have that  $\lambda_c = 0.32$  devices/km, which means that the density of devices per square kilometre needs only to be greater than  $\lambda_c \gamma = 6.4$  devices/km<sup>2</sup>, while if  $r = 0.075\text{km}$ , it should be greater than 300 devices/km<sup>2</sup>. For a rural area,  $\gamma \approx 1\text{km}^{-1}$ , if  $r = 0.3\text{km}$ , the number of devices per kilometre of streets must be greater than 12 to have percolation.

We can see here that the results are very near to the PBM for high values of  $r\gamma$ , which means that in the limit of dense streets with a reasonable interaction radius, the street system does not play a role and the Cox point process is near to a planar Poisson point process. On the other hand, when the street system becomes sparse, for low values of  $r\gamma$ , the PBM is not a good approximation. An inhomogeneous Bernoulli bond percolation model can be used for approximations, for details see [12]. In the case of PVT, the critical Bernoulli parameter can be approximated by  $b_c = 0.5$ , resulting in the approximation

$$\lambda_c/\gamma \exp(-r\lambda_c) = -\log(b_c).$$

This gives  $\lambda_c/\gamma \approx 12$  devices which is very close to the value found for  $r\gamma = 0.3$  in the simulations.

The simulations also show that the transition from the approximation by the PBM to the approximation by the inhomogeneous Bernoulli bond percolation is very steep, which means that almost all values of  $r\gamma$  can be covered by one of the two approximations presented. This also gives us the domain of validity for each approximation.

### B. Estimation of the percolation probability

The simulation method for the percolation probability  $\theta$  follows the algorithm described in Section III-B. Again, the tessellation is traced and the devices placed on a torus. For each value of  $r\gamma$ , the estimates are based on  $N = 10$  realisations of the random tessellation and  $M = 30$  realisations

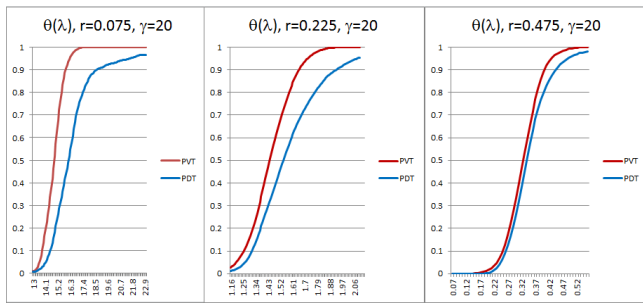


Fig. 5: Percolation probability as a function of intensity for varying communication radii.

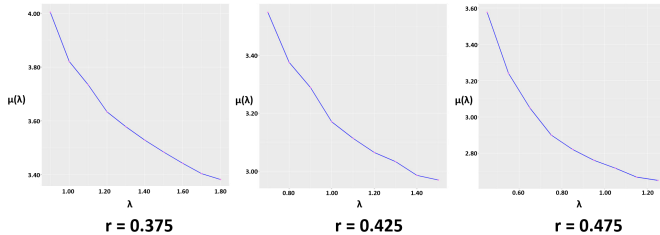


Fig. 6: Stretch factor for PVT as a function of intensity for varying communication radii.

of randomly placed devices on each of these tessellations. The results are presented in Figure 5. The  $\theta$  curve gives the probability for a randomly selected user to belong to the infinite connected component. The curves have been calculated for various values of  $r\gamma$ . Thus, for big interaction radii, both PDT and PVT model are very close to the standard PBM, while for smaller radii, the percolation probability is always smaller for PDT than for PVT.

The curves show the significant difference appearing between PDT and PVT models when  $r\gamma$  becomes small. In the PDT model, the percolation probability  $\theta$  increases much more slowly. In particular, even far above the percolation threshold, some devices are not connected to the network.

### C. Estimation of the stretch factor

Here, the window is  $5\text{km} \times 5\text{km}$  and again the tessellations and devices are traced on a torus. In order to estimate the stretch factor  $\mu$ , the values of  $\lambda$  are taken above the critical value, and only devices in the infinite connected component are taken into account. For each value of  $\lambda$ , 100 simulations are performed. Figures 6 and 7 illustrate the results with  $\gamma = 20\text{km}^{-1}$  and varying  $r$ . For instance in PVT with  $r = 0.375\text{km}$  and  $\lambda = 1.5$  devices/km, if two devices in the infinite connected component are at distance  $2\text{km}$ , then approximately 7 hops are required. Additionally, note that the stretch factor is bigger for PDT than for PVT.

## V. CONCLUSION

The results obtained in this paper are a first step towards analysing connectivity in multi-hop wireless networks. For

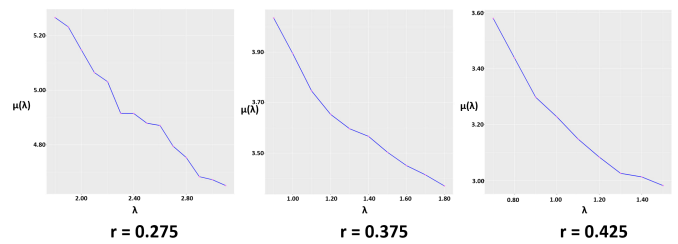


Fig. 7: Stretch factor for PDT as a function of intensity for varying communication radii.

rural areas, where shadowing and interferences have little impact, the model already covers a large proportion of pertinent features. It reveals that the inhomogeneous Bernoulli bond percolation model gives a much better approximation for these type of areas than the PBM. Even more, it shows that in rural areas, for PDT models, the percolation probability will stay far from 1. Although realistic models for urban areas will need to take into account the propagation effects caused by the urban landscape, the proposed model already gives strong hints on methods for addressing the basic problem of connectivity.

Dealing with shadowing in urban areas now seems to be a reasonable next step. One idea that we are currently exploring is to introduce a reduced connection radius for points that do not belong to the same street segment. Moreover, other street system models, like Manhattan grids, or embedded tessellations could also be studied in order to represent a larger class of real world street systems.

## ACKNOWLEDGMENTS

This research was supported by the Leibniz program *Probabilistic Methods for Mobile Ad-Hoc Networks*, by the LMU Munich's Institutional Strategy LMUexcellent within the framework of the German Excellence Initiative and by Orange S.A. grant CRE G09292.

## REFERENCES

- [1] A. Asadi, Q. Wang, and V. Mancuso, "A survey on device-to-device communication in cellular networks," *IEEE Commun. Surveys Tuts.*, vol. 16, no. 4, pp. 1801–1819, 2014.
- [2] P. Gandotra, R. K. Jha, and S. Jain, "A survey on device-to-device (D2D) communication: Architecture and security issues," *J. Netw. Comput. Appl.*, 2016.
- [3] I. Glauche, W. Krause, R. Sollacher and M. Greiner, "Continuum percolation of wireless ad hoc communication networks," *Phys. A*, vol. 325, no. 3, pp. 577–600, 2003.
- [4] E. Sporadev, *Stochastic Geometry, Spatial Statistics and Random Fields*, ser. Lecture Notes in Mathematics, vol. 2068. Berlin: Springer, 2013.
- [5] R. Maier and V. Schmidt, "Stationary iterated tessellations," *Adv. Appl. Prob.*, vol. 35, no. 3-4, pp. 337–353, 2003.
- [6] C. Gloaguen, F. Fleischer, H. Schmidt and V. Schmidt, "Fitting of stochastic telecommunication network models via distance measures and Monte-Carlo tests," *Telecommun. Syst.*, vol. 31, no. 4, pp. 353–377, 2006.
- [7] C. Gloaguen, F. Voss and V. Schmidt, "Parametric distance distributions for fixed access network analysis and planning," in *ITC21 (21st International Teletraffic Congress)*, Paris, 2009.
- [8] C. Gloaguen and E. Cali, "Cost estimation of a fixed network deployment over an urban territory," *Annals of Telecommunications*, 2017. [Online]. Available: <https://doi.org/10.1007/s12243-017-0614-3>

- [9] R. Meester and R. Roy, *Continuum Percolation*. Cambridge University Press, Cambridge, 1996.
- [10] T. Courtat, "Promenade dans les cartes de villes -phénoménologie mathématique et physique de la ville- une approche géométrique," Ph.D. dissertation, Université Paris-Diderot, Paris, 2012.
- [11] S.N. Chiu, D. Stoyan, W.S. Kendall and J. Mecke, *Stochastic Geometry and Its Applications*. Chichester: J. Wiley and Sons, 2013.
- [12] C. Hirsch, B. Jahnel, and E. Cali, "Continuum percolation for Cox point processes," *arXiv preprint arXiv:1710.11407*, 2017.
- [13] C.-L. Yao, G. Chen, and T.-D. Guo, "Large deviations for the graph distance in supercritical continuum percolation," *J. Appl. Probab.*, vol. 48, no. 1, pp. 154–172, 2011.
- [14] S. Mertens and C. Moore, "Continuum percolation thresholds in two dimensions," *Phys. Rev. E*, vol. 86, no. 6, pp. 061–109, Dec. 2012.
- [15] R.W. Floyd, "Algorithm 97 : shortest path," *Communications of the ACM*, vol. 5, no. 6, p. 345, Jun. 1959.
- [16] R Development Core Team, *R: A Language and Environment for Statistical Computing*, R Foundation for Statistical Computing, Vienna, 2008.
- [17] P. Balister, B. Bollobás, and M. Walters, "Continuum percolation with steps in the square or the disc," *Random Structures Algorithms*, vol. 26, no. 4, pp. 392–403, 2005.